

**Metallic atomic wires on patterned dihydrogenated Si(001)**

Bikash C. Gupta and Inder P. Batra

*Department of Physics, University of Illinois at Chicago, 845 West Taylor Street, Chicago, Illinois 60607-7059, USA*

(Received 24 November 2004; published 26 April 2005)

Electronic structure calculations are performed for atomic wires of metals like Al, Ga, and In placed on a patterned dihydrogenated Si(001): $1 \times 1$  in search of structures with metallic behavior. The dihydrogenated Si(001) is patterned by de-passivating hydrogen atoms only from one row of Si atoms along the  $[1\bar{1}0]$  direction. Various structures of adsorbed metals and their electronic properties are examined. It is found that Al and Ga atomic wires with metallic property are strongly unstable towards the formation of buckled metal dimers leading to semiconducting behavior. Indium atomic wire, however, displays only marginal preference towards the formation of symmetric dimers staying close to the metallic limit. The reasons behind the lack of metallic atomic wires are explored. In addition, a direction is proposed for the realization of metallic wires on the dihydrogenated Si(001).

DOI: 10.1103/PhysRevB.71.165429

PACS number(s): 73.20.-r, 73.21.Hb, 73.90.+f

**I. INTRODUCTION**

The study of metals on semiconductors dates back to the nineteenth century and has seen a vigorous recent revival due to tremendous interest in nanotechnology. The scanning tunneling microscopy has enabled us to manipulate atoms, and place them at will on different surface sites to create exotic artificial atomic scale structures with interesting electronic properties.<sup>1-4</sup> The placement of metal atoms such as Al, Ga, and In on Si(001) may lead to the formation of low-dimensional structures,<sup>5</sup> exhibiting significant electronic and transport properties. Atomic scale structures themselves have technological applications in developing atomic scale devices.<sup>6</sup> In particular, realization of a one-dimensional (1D) metallic nanowire is of great importance because of its possible use as metallic interconnect in nanodevices.

There is much current activity in a bottom-up approach where free standing atomic and nanowires for a variety of atoms, e.g., K, Al, Cu, Ni, Au, and Si, have been studied.<sup>7-14</sup> The geometrical structures of such free standing wires and their electronic properties have been discussed. A general finding is that a zigzag structure in the form of an equilateral triangle is most stable.<sup>7,8,12,14</sup> This can be understood as arising primarily due to the maximization of coordination number for each atom in a quasi-1D structure. Another structure, a local minimum on energy surface, but not terribly stable, is a wide angle isosceles triangle which somehow is reminiscent of the bulk environment. For example, Si which is four-fold coordinated in the bulk (tetrahedral angle  $\sim 109^\circ$ ) shows<sup>14</sup> a local minimum at an angle of  $\sim 117^\circ$  going towards  $sp^2$  configuration. In general, free standing atomic wires tend to be metallic (have bands crossing the Fermi level) but these wires in practice have to be supported. Silicon is the most widely used substrate for practical applications and the low index surfaces, Si(001) is the surface of choice. With the downward spiral toward nanodevices, it is desirable to investigate the electronic properties at the lowest possible coverages. It is in this context that the study of metals like Al, Ga, and In at submonolayer coverages on Si(001) takes on the added importance. The interaction of metal nanowires with substrate can significantly alter the

electronic properties, and not always in the desired direction.

There continues to be a persistent search for metallic nanowires on clean Si(001): $2 \times 1$  surface as well as on the hydrogen terminated Si(001): $2 \times 1$  surface.<sup>4,15-20</sup> In an early study,<sup>15</sup> Batra proposed the formation of a zigzag atomic chain of Al on Si(001): $2 \times 1$  but energetically it was not the most favored structure. In more recent studies, it was shown that the zigzag Al chain is hard to fabricate as it is energetically 1.6 eV higher than the most favorable structure. However, our spin-restricted calculations for this chain indicate no Peierls distortion and hence the chain remains semimetallic in character.<sup>16</sup>

Recently, the hydrogen terminated Si(001) has become one of the surfaces of choice for growing atomic scale structures. The hydrogen terminated Si(001) can have various reconstructed patterns such as  $2 \times 1$ ,  $3 \times 1$ , and  $1 \times 1$  depending on the hydrogen coverage and the experimental environment.<sup>21-27</sup> Watanabe *et al.*<sup>19</sup> explored the growth of Ga on the patterned monohydride Si(001): $2 \times 1$ . Using STM tip a monohydride Si(001) may be patterned by removing hydrogen atoms on a chosen row of surface Si atoms either along  $[1\bar{1}0]$  or  $[110]$  direction. Watanabe and co-workers<sup>19,20</sup> examined several possible structures of Ga on such a patterned monohydride Si(001): $2 \times 1$  surface and they found one-dimensional structures made of small Ga clusters. However, the structures turned out to be either semimetallic or semiconducting.

It has been shown in an experiment that an ideal hydrogen terminated Si(001): $1 \times 1$  surface can be achieved by wet-chemical etching.<sup>27</sup> Furthermore, it is known that with the help of a STM tip, some selected hydrogen atoms from the surface can be desorbed. We therefore explore the adsorption of Al, Ga, and In on a patterned dihydrogenated Si(001): $1 \times 1$  where Si atoms on a single row along the  $[1\bar{1}0]$  direction are de-passivated. In other words, the Si atoms on a single row along the  $[1\bar{1}0]$  direction have two dangling bonds each while all other Si atoms on the surface are saturated with hydrogen atoms. Various possible structures for Al, Ga, and In on the dihydrogenated Si(001): $1 \times 1$  and their properties are studied and a direction is proposed for the realization of

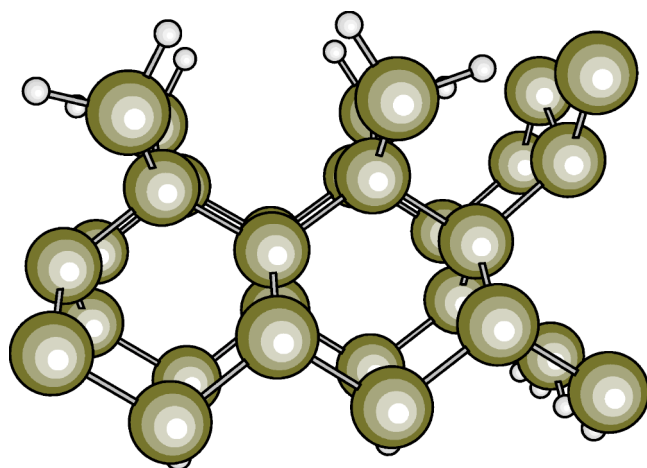


FIG. 1. Silicon and hydrogen atoms within the supercell ( $3 \times 2$ ) for the patterned dihydrogenated Si(001): $1 \times 1$ . The large and small circles represent Si and hydrogen atoms, respectively. The top layer Si atoms on the rightmost row have two dangling bonds each as they are not passivated by hydrogen atoms.

a metallic atomic wire on the dihydrogenated Si(001): $1 \times 1$ .

## II. METHOD

First-principle total-energy calculations were carried out within the density-functional theory at zero temperature using the VASP code.<sup>28</sup> The wave functions are expressed by plane waves with the cutoff energy  $|k+G|^2 \leq 250$  eV. The Brillouin zone (BZ) integrations are performed by using the Monkhorst-Pack scheme with  $4 \times 4 \times 1$   $k$ -point meshes for  $3 \times 2$  primitive cells. Ions are represented by ultrasoft Vanderbilt-type pseudopotentials and results for fully relaxed atomic structures are obtained using the generalized gradient approximation (GGA). The preconditioned conjugate gradient method is used for the wave-function optimization and the conjugate gradient method for ionic relaxation.

The Si(001) surface is represented by a repeated slab geometry. Each slab contains five Si atomic planes. The bottom layer Si atoms are passivated by hydrogen atoms. In addition, within the supercell, two consecutive rows of Si atoms extending along the  $[1\bar{1}0]$  direction on the top layer are passivated with hydrogen atoms (see Fig. 1). Consecutive slabs are separated by a vacuum space of 9 Å. The Si atoms on the top four layers of the slab and hydrogen atoms attached to top layer Si atoms are allowed to relax while Si atoms in the bottom layer of the slab and the passivating hydrogen atoms are kept fixed to simulate the bulklike termination. The convergence with respect to the energy cutoff and the number of  $k$  points for similar structures has been examined earlier.<sup>16</sup>

## III. RESULTS AND DISCUSSIONS

The lowest energy structure of the patterned dihydrogenated Si(001) surface is shown in Fig. 1. The surface retains its unit periodicity along the  $y[1\bar{1}0]$  direction. The unsaturated Si atoms on the surface (third row of Si atoms on the top layer in Fig. 1) forms a dangling bond wire extending along

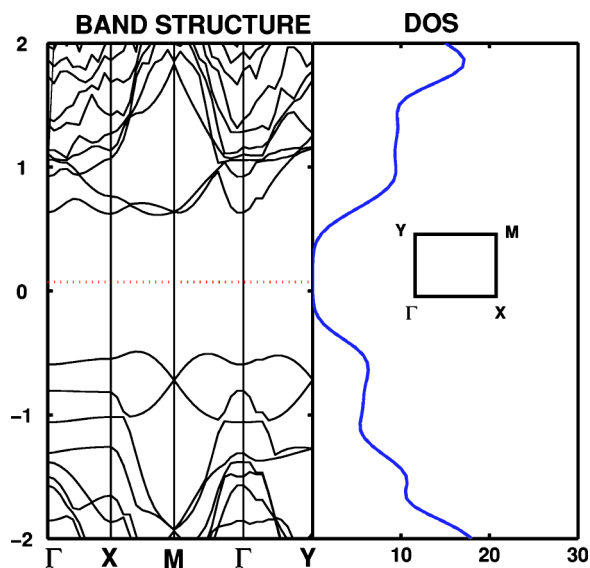


FIG. 2. Band structure (left panel) and density of states (right panel) for the patterned dihydrogenated Si(001) surface shown in Fig. 1. The dotted line represents the Fermi level. The  $\Gamma$ , X, M, and Y points are shown in the inset of the right panel.

the  $y$  direction. Figure 2 shows the band structure (left panel) and the density of states (right panel) for the dangling-bond wire. In all the band structure plots we have scaled  $K_x$  and  $K_y$  by  $\pi/3a$  and  $\pi/2a$ , respectively. A wide band gap ( $\sim 1.3$  eV) around the Fermi level indicates that the surface is semiconducting in nature. The band gap is reflected in the density of states plot with vanishing density of states around the Fermi level. This is in contrast to the metallic nature of dangling-bond wire on monohydride Si(001): $2 \times 1$  surface.<sup>19,20</sup>

Metal atoms are adsorbed on the surface shown in Fig. 1 to examine the possibility of the formation of a metallic nanowire supported on the Si substrate. Experiments have shown that the Al and Ga atoms can diffuse easily<sup>5,29</sup> on the hydrogen terminated surface and therefore the exposed Al, Ga, and In atoms are expected to diffuse and nucleate around the Si dangling bonds on the surface. Thus it may be possible to form a nanowire of metal atoms supported on the substrate. We are in search of a supported atomic wire that will be metallic in character. The adsorption of metals like Al, Ga, and In is studied as a part of this search.

Here we consider the Al adsorption on the patterned dihydrogenated Si(001) surface shown in Fig. 1. The surface offers various possible sites for the Al adsorption. Two different kinds of sites are denoted by  $S$  ( $S_1$  or  $S_2$ ) and  $P$  ( $P_1$  or  $P_2$ ), respectively as shown in Fig. 3. The sites vertically above the hydrogen free Si atoms (Si atoms with dangling bonds) are denoted as  $T$  ( $T_1$  or  $T_2$ ). The configurations considered here are  $T_1T_2$  (one Al is placed on top of the Si atom marked as 1 and the other Al atom is placed on top of the Si atom marked as 2),  $S_1S_2$  (one Al is placed at  $S_1$  site and the other one is placed at  $S_2$  site) and  $P_1P_2$  (one Al is placed at  $P_1$  site and the other is placed at  $P_2$  site) respectively. For the  $T_1T_2$  configuration, the Al atoms are allowed to move along the  $z$  direction only, this configuration is found to be least

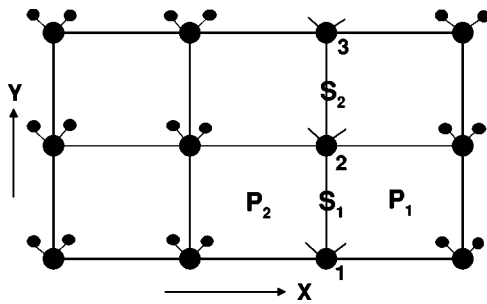


FIG. 3. Schematic representation of the atomic positions on the top of the slab within the supercell. Small circles represent the hydrogen atoms on the top of the slab and large circles represent the first layer Si atoms. The Si atoms with dangling bonds are marked as 1, 2, and 3, respectively. The sites  $S_1$  and  $S_2$  have identical surrounding and similarly sites  $P_1$  and  $P_2$  have identical environment.

favorable. The total energies of other configurations are calculated with respect to the total energy for the  $T_1T_2$  configuration. The  $S_1S_2$  and  $P_1P_2$  configurations are more favorable than the  $T_1T_2$  by 0.42 and 0.71 eV, respectively. The  $S_1S_2$  configuration is interesting because the band structure and the density of states (see Fig. 4) for this structure indicate the metallic behavior of Al atomic wire extending along the  $y$  direction. On the other hand, the Al structure with the  $P_1P_2$  configuration shows nonmetallic behavior (see a band gap around the Fermi level in Fig. 5). For the  $S_1S_2$  configuration, each Al atom forms two bonds with two Si atoms (each Si-Al bond length is  $\sim 2.6$  Å) and the surface retains its unit periodicity along the  $y$  direction. Therefore the single free electron of the Al atom in the unit cell is responsible for the partially filled bands crossings through the Fermi level. Consequently the density of states increases around the Fermi level and the atomic wire (with  $S_1S_2$  configuration) is metallic in character. For the  $P_1P_2$  configuration, we note that Al

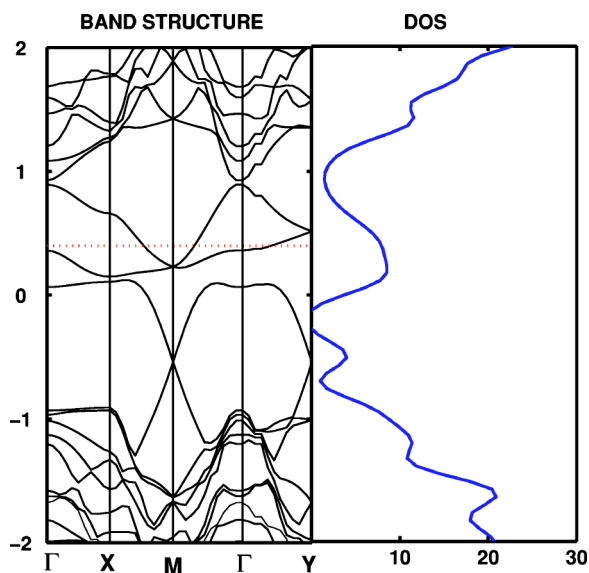


FIG. 4. The band structure (left panel) and the density of states (right panel) corresponding to the  $S_1S_2$  configuration of Al. The dotted line shows the Fermi level.

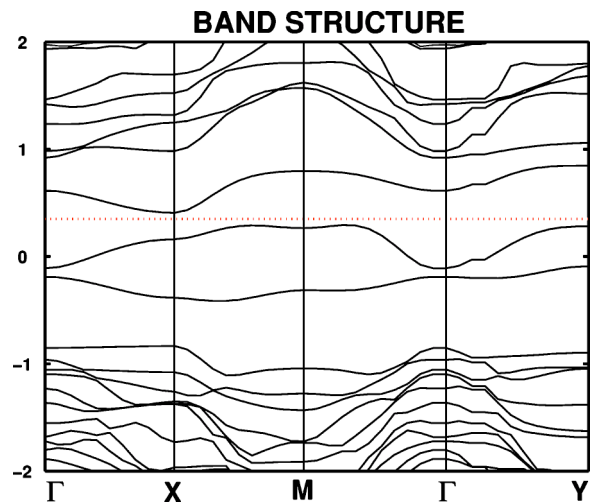


FIG. 5. The band structure corresponding to the  $P_1P_2$  configuration of Al. The Fermi level is indicated by the dotted line.

atoms make strong bonds with Si atoms (bond length  $\sim 2.5$  Å while they fail to make a bond among themselves (distance between two Al atoms  $\sim 3.2$  Å). In this configuration, the periodicity along the  $y$  direction is doubled compared to that for the  $S_1S_2$  configuration. Two electrons from two Al atoms become nonitinerant in the unit cell, prefer to be occupied by a single band, and hence the Al structure (with  $P_1P_2$  configuration) extending along the  $y$  direction becomes nonmetallic. Similar to the zigzag Al chain considered earlier<sup>15,16</sup> on the bare Si(001): $2 \times 1$ , we also considered a zigzag Al chain configuration by displacing the Al atom at  $S_1$  site by  $\Delta$  along the positive  $x$  direction and the Al atom at  $S_2$  site by  $\Delta$  along the negative  $x$  direction. This zigzag chain configuration turned out to be unstable and readily reverted to the  $S_1S_2$  configuration.

However, the most favorable configuration is the one where the Al atom at the  $S_1$  site is shifted along the positive  $y$  direction by  $0.2$  Å while that at the  $S_2$  is shifted along the negative  $y$  direction by  $1.6$  Å to form a buckled Al dimer ( $\Delta z \approx 0.8$  Å) with a bond length of  $\sim 2.6$  Å. The buckled Al dimers can be seen in the charge-density plot in Fig. 6A where the large circles represent Al atoms while the small circles represent Si atoms (just below the Al wire). We will call this configuration the Al-dimer configuration which has a behavior akin to the buckled Si dimer on Si (001). This is clear from the charge-density plot in Fig. 6A. The total energy of this configuration is  $-0.94$  eV compared to the  $T_1T_2$  configuration, i.e., this Al-dimer configuration is favorable over the  $S_1S_2$  configuration by  $0.52$  eV. This energy is gained mostly due to the optimization of Al-Si bonds. The nature of the Al wire extending along the  $y$  direction becomes nonmetallic as can be seen from the band structure with an energy gap around the Fermi level [see Fig. 6B]. We therefore conclude that the metallic Al nanowire [corresponding to the configuration  $S_1S_2$  on the dihydrogenated Si(001)] cannot be achieved.

We next consider the Ga adsorption on the same patterned dihydride Si(001). It is known that at some coverages, Ga behaves in a different way compared to Al.<sup>16</sup> The  $T_1T_2$  con-



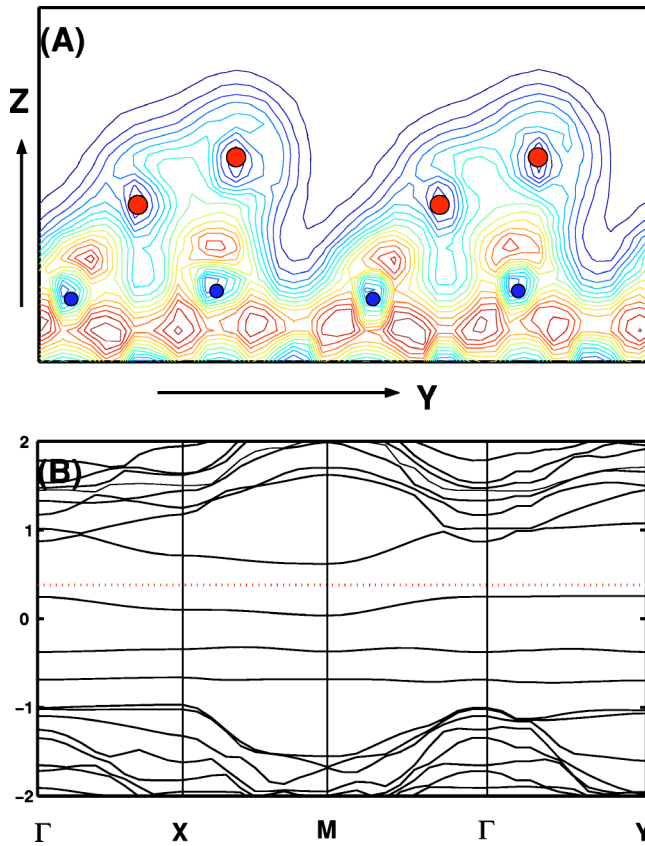


FIG. 6. This corresponds to the most favorable Al-dimer configuration: (A) The charge density plot on the  $y$ - $z$  plane including the Al atoms and (B) the band structure where the dotted line indicates the Fermi level.

figuration is the least favorable one. However, unlike the case of Al, the  $S_1S_2$  configuration for Ga (total energy  $-0.41$  eV compared to the  $T_1T_2$  configuration) is only slightly more favorable by  $0.02$  eV compared to the  $P_1P_2$  configuration. The Ga atomic wire with the  $S_1S_2$  configuration is metallic in character with a peak for density of states around the Fermi level (see Fig. 7). However, the most stable configuration is very similar to that we found for Al. Two Ga atoms form a buckled dimer as can be seen from the charge-density plot in Fig. 8A (the large circles represent the Ga atoms and the small circles represent Si atoms just below the Ga atoms). This most favorable configuration is denoted as the Ga-dimer configuration. The atomic wire made of buckled Ga dimers extending along the  $y$  direction is nonmetallic in nature and this can be seen from the band-structure plot in Fig. 8B. Similar to the Al case, we therefore conclude that stable metallic Ga wire cannot be realized on patterned dihydrogenated Si(001). We, however, notice that the total-energy difference between the Ga-dimer configuration and the  $S_1S_2$  configuration is  $0.41$  eV which is lower by  $0.1$  eV compared to that for the Al case. The reduction in the total-energy difference between the  $S_1S_2$  and dimer configuration for Ga encourages us to study the In adsorption on the same patterned dihydrogenated Si(001).

Unlike the case of Al and Ga the  $P_1P_2$  is the least favorable configuration for In. The total energy for this configu-

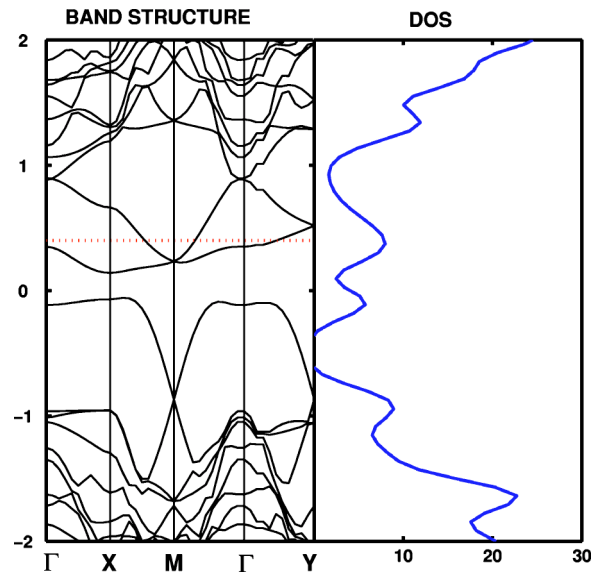


FIG. 7. The band structure (left panel) and the density of states (right panel) corresponding to the  $S_1S_2$  configuration of Ga. The Fermi level is shown by the dotted line.

ration compared to the  $T_1T_2$  configuration is  $+0.08$  eV. The total energy for the  $S_1S_2$  configuration compared to the  $T_1T_2$  configuration is  $-0.20$  eV. The In atomic wire with the  $S_1S_2$  configuration is metallic in character with large density of states around the Fermi level and this can be seen from the band structure (left panel) and density of states (right panel)

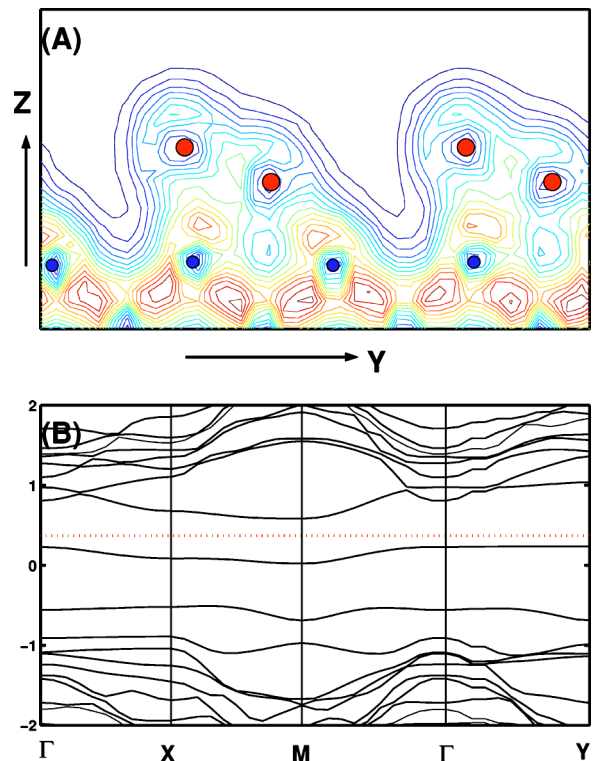


FIG. 8. This corresponds to the most favorable configuration of Ga (Ga-dimer configuration): (A) The charge-density plot on the  $y$ - $z$  plane including the Ga atoms and (B) the band structure where the Fermi level is indicated by the dotted line.

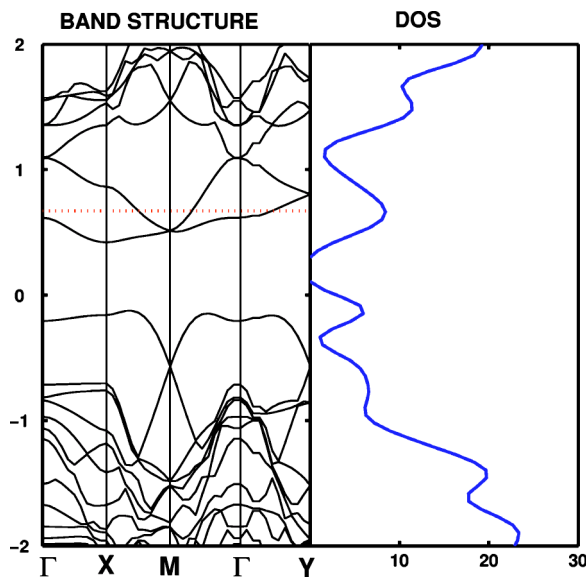


FIG. 9. The band structure (left panel) and the density of states (right panel) corresponding to the  $S_1S_2$  configuration of In. The Fermi level is represented by the dotted line.

plot in Fig. 9. The most favorable configuration for In is a nonbuckled In dimer as seen from the charge-density plot in Fig. 10A where the In atoms (large circles in the figure) at  $S_1$  and  $S_2$  positions move towards each other by 0.3 Å to form a weak dimer. Consequently, the nanowire consisting of unbuckled weak In dimers becomes nonmetallic [see the band structure in Fig. 10B]. We note that the total energy for this configuration is  $-0.27$  eV which is more favorable compared to the  $S_1S_2$  configuration only by 0.07 eV. At room temperature the thermal energy is expected to be sufficient to break these weak dimer bonds leading to metallic behavior of In wires on the dihydrogenated Si(001). Here we add that there are situations where the experimentally observed structure corresponds to some local minimum-energy structure.<sup>16,30</sup> Therefore an experiment on this system is desirable to confirm if the In atomic wire can be realized.

#### IV. CONCLUSION

First-principle electronic structure calculations are performed to examine the possibility for the formation of stable metallic atomic wires on the dihydrogenated Si(001). Adsorption of metals like Al, Ga, and In are considered for this

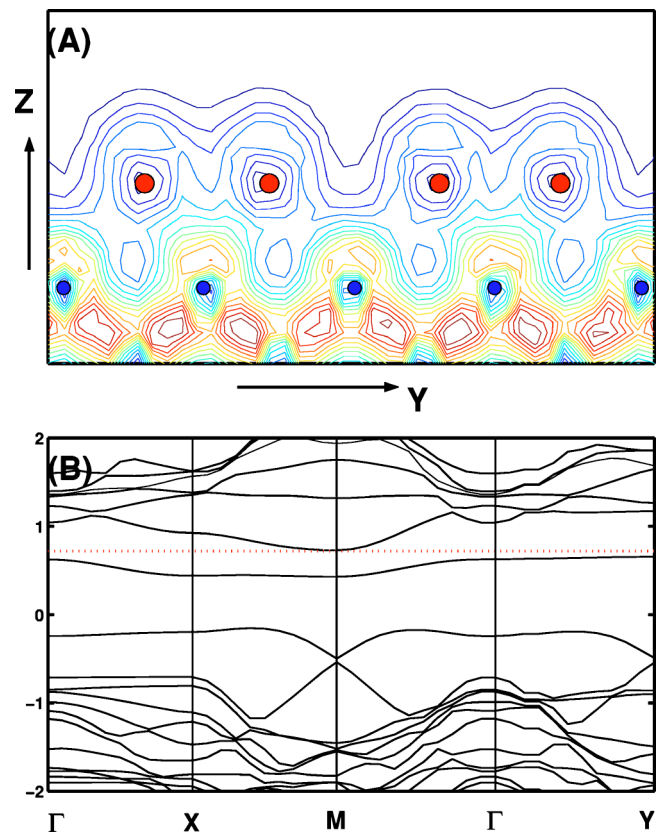


FIG. 10. This corresponds to the most favorable configuration for In: (A) The charge-density plot on the  $y$ - $z$  plane including the In atoms and (B) The band structure; dotted line represents the Fermi level.

purpose. We found that the Al and Ga nanowire configurations with metallic character are unstable towards the formation of buckled metal dimers leading to semiconducting behavior. However, the metallic In wire is weakly unstable because the total energy corresponding to the metallic wire configuration is very close to the most favorable nonmetallic (weakly dimerized) configuration. The thermal energy may be able to break the weak bonds between In atoms and thus a metallic In wire may be realized on Si(001). Our results indicate that as we go from Al to In via Ga, the metallic nanowire configuration approaches towards the most favorable one. We are hopeful that this work will encourage further experimental studies of In atomic wires on a patterned dihydrogenated Si(001).

<sup>1</sup>S. Hosoki, S. Hosaka, and T. Hasegawa, *Appl. Surf. Sci.* **60**, 643 (1992).

<sup>2</sup>M. F. Crommie, C. P. Lutz, and D. M. Eigler, *Science* **262**, 218 (1993).

<sup>3</sup>T. -C. Shen, C. Wang, G. C. Abeln, J. R. Tucker, J. W. Lyding, Ph. Avouris, and R. E. Walkup, *Science* **268**, 1590 (1995).

<sup>4</sup>*Advances in Scanning Probe Microscopy*, edited by T. Sakurai and Y. Watanabe (Springer-Verlag, Berlin, 1989).

<sup>5</sup>T. -C. Shen, C. Wang, and J. R. Tucker, *Phys. Rev. Lett.* **78**, 1271 (1997).

<sup>6</sup>Y. Wada, T. Uda, M. Lutwyche, S. Kondo, and S. Heike, *J. Appl. Phys.* **74**, 7321 (1993).

<sup>7</sup>D. S. Portal, E. Atracho, J. Junquera, P. Ordenjon, and J. M. Soler, *Phys. Rev. Lett.* **83**, 3884 (1999).

<sup>8</sup>D. S. Portal, E. Atracho, J. Junquera, A. Garcia, and J. M. Soler, *Surf. Sci.* **482-485**, 1261 (2001).

- <sup>9</sup>J. A. Torres, E. Tosatti, A. D. Coros, F. Ercolessi, J. J. Kohanoff, F. D. Di Tolla, and J. M. Soler, *Surf. Sci.* **426**, L441 (1999).
- <sup>10</sup>M. Okamoto and K. Takayanagi, *Phys. Rev. B* **60**, 7808 (1999).
- <sup>11</sup>H. Hakkinen, R. N. Barnett, U. Landman, *J. Phys. Chem. B* **103**, 8814 (1999); H. Hakkinen, R. N. Barnett, A. G. Scherbakov, U. Landman, *ibid.* **104**, 9063 (2000).
- <sup>12</sup>P. Sen, S. Ciraci, A. Budlum, and I. P. Batra, *Phys. Rev. B* **64**, 195420 (2001).
- <sup>13</sup>P. Sen, O. Glseren, T. Yildirim, I. P. Batra, and S. Ciraci, *Phys. Rev. B* **65**, 235433 (2002).
- <sup>14</sup>I. P. Batra, T. Ciani, D. Boddupalli, and L. Soberano, *Technical Proceedings of the 2003 Nanotechnology Conference and Trade Show, San Francisco, 2003* (Computational Publications, Cambridge MA), Vol. 2, p. 206.
- <sup>15</sup>I. P. Batra, *Phys. Rev. Lett.* **63**, 1704 (1989).
- <sup>16</sup>B. C. Gupta and I. P. Batra, *Phys. Rev. B* **69**, 165322 (2004); see also *Phys. Rev. B* **68**, 045409 (2003).
- <sup>17</sup>J. N. Crain, A. Kirakosian, K. N. Altmann, C. Bromberger, S. C. Erwin, J. L. McChesney, J.-L. Lin, and F. J. Himpsel, *Phys. Rev. Lett.* **90**, 176805 (2003).
- <sup>18</sup>J. N. Crain, J. L. McChesney, Fan Zheng, M. C. Gallagher, P. C. Snijders, M. Bissen, C. Gundelach, S. C. Erwin, and F. J. Himpsel, *Phys. Rev. B* **69**, 125401 (2004).
- <sup>19</sup>S. Watanabe, Y. Ono, T. Hashizume, and Y. Wada, *Phys. Rev. B* **54**, R17308 (1996).
- <sup>20</sup>S. Watanabe, M. Ichimura, T. Onogi, and Y. Ono, *Jpn. J. Appl. Phys., Part 2* **36**, L929 (1997).
- <sup>21</sup>J. J. Boland, *Adv. Phys.* **42**, 129 (1993).
- <sup>22</sup>F. S. Tautz and J. A. Schaefer, *J. Appl. Phys.* **84**, 6636 (1998).
- <sup>23</sup>Y. J. Chabal and K. Raghavachari, *Phys. Rev. Lett.* **54**, 1055 (1985).
- <sup>24</sup>J. J. Boland, *Phys. Rev. Lett.* **65**, 3325 (1990).
- <sup>25</sup>J. J. Boland, *Surf. Sci.* **261**, 17 (1992).
- <sup>26</sup>Y. J. Chabal and K. Raghavachari, *Phys. Rev. Lett.* **53**, 282 (1984).
- <sup>27</sup>Y. Morita and H. Tokumoto, *Appl. Phys. Lett.* **67**, 2654 (1995); *J. Vac. Sci. Technol. A* **14**, 854 (1995).
- <sup>28</sup>G. Kresse and J. Hafner, *Phys. Rev. B* **47**, R558 (1993); G. Kresse and J. Furthmuller, *ibid.* **54**, 11 169 (1996).
- <sup>29</sup>T. Hashizume, S. Heike, M. I. Lutwyche, S. Watanabe, K. Nakajima, T. Nishi, and Y. Wada, *Jpn. J. Appl. Phys., Part 2* **35**, L1085 (1996).
- <sup>30</sup>B. Bourguignon, K. L. Cerleton, and S. R. Leone, *Surf. Sci.* **204**, 455 (1988).